

# Progress on three-dimensional visualizing skin architecture with multiple immunofluorescence staining and tissue-clearing approaches

Yuqing Wang, Wanzhu Bai and Xiaoyu Wang

Institute of Acupuncture and Moxibustion, China Academy of Chinese Medical Sciences, Beijing, China

**Summary.** The skin forms the external covering of the body and is its largest organ, comprising many different cell types. Although the diversity of these cells has been widely studied with various histological methods, our understanding of skin architecture is mainly established on thin tissue sections, which restricted the information available to two dimensions. The development of innovative techniques to induce optical transparency (“clearing”) in biological tissues has enabled researchers to visualize the three-dimensional reconstruction of intact organs and thick tissue sections at a cellular resolution. With the aid of tissue-clearing treatment, the labeled cutaneous nerve fibers and blood vessels can be followed for a longer distance on the thicker skin section or the whole mount skin under a fluorescence microscopy or a confocal microscopy. It is beneficial for demonstrating the morphological characteristics of nerve fibers and blood vessels themselves, as well as their spatial interconnection. In this review, we provide a brief summary of the literature on the use of tissue optical clearing methods and describe our experience of multiple fluorescent staining and tissue clearing approaches on thicker skin sections and whole-mount skin in our laboratory. Given the existing conventional methods, we expected to provide a more effective approach to comprehensively study skin architecture.

**Key words:** Blood vessels, Fluorescent labeling, Histology, Nerve fibers, Three-dimensional reconstruction, Tissue clearing

## Introduction

Skin tissue is a complex and highly specialized organ, consisting of multiple layers and diverse cell types with distinct characteristics and functions that serve essential functions related to its external surface location in the body. It is known to comprise orderly arranged layers of epidermis, dermis, and hypodermis (subcutaneous tissue) that are not only composed of their corresponding cellular constituents, such as epithelial cells, keratinocytes, Langerhans cells, etc., but also with long-ranged nerve fibers, blood vessels, and lymphatic vessels distributed throughout. These cellular constituents and tissue structures are highly organized to perform a wide range of functions, including protection, temperature regulation, sensation, and immune defense. However, our information is two-dimensional from thin tissue sections with conventional histological approaches (Navarro et al., 1995; Pomaville and Wright, 2021). Recently, with the development of imaging techniques such as laser confocal microscopy, multiphoton microscopy, and light-sheet fluorescence microscopy, numerous tissue-clearing methods for improving optical access and depth of imaging in thick tissue, whole organs, and intact bodies have emerged (Susaki and Ueda, 2016; Tian and Li, 2020). Taking advantage of them, it becomes possible to investigate skin architecture with a three-dimensional view (Wang et al., 2022; Zhang et al., 2023).

## Development and application of tissue-clearing methods

Tissue-clearing methods primarily rely either on organic solvent- or hydrophilic reagent-clearing solutions to mitigate light scattering caused by heterogeneous cellular constituents with different refractive indices within tissues under the fluorescence microscopy (Richardson and Lichtman, 2015). CLARITY (clear lipid-exchanged acrylamide hybrid rigid imaging/immunostaining compatible tissue

*Corresponding Author:* Xiaoyu Wang, Institute of Acupuncture and Moxibustion, China Academy of Chinese Medical Sciences, 16 Nanxiaojie of Dongzhimennei, Beijing, 100700, PR China. e-mail: xiaorain\_wang@hotmail.com  
www.hh.um.es. DOI: 10.14670/HH-18-815



hydrogel) is a tissue-clearing technology that emerged in 2013 (Chung et al., 2013). Then, many protocols were originally applied to the central nervous system and whole embryos, including three-dimensional imaging of solvent-cleared organs (3DISCO) (Ertürk et al., 2012), see deep brain (SeeDB) (Ke et al., 2013), clear unobstructed brain imaging cocktails (CUBIC) (Susaki et al., 2014), passive clarity technique (PACT) (Yang et al., 2014), ultimate DISCO (uDISCO) (Pan et al., 2016), and RapiClear (Bekkouche et al., 2020). Recent refinements in tissue-clearing techniques have facilitated exceptional optical access to many other mammalian tissues (Tian et al., 2021).

Tissue-clearing methods can be broadly classified based on their underlying principles and techniques. Here is a classification of tissue-clearing methods: 1) Hydrophilic (Chung and Deisseroth, 2013; Zhu et al., 2019; Peng et al., 2022): these methods focus on making tissues transparent by replacing water within the tissue with hydrophilic agents-e.g., CLARITY; 2) Hydrophobic (Renier et al., 2014; Pan et al., 2016; Kirchner et al., 2020): these methods rely on hydrophobic agents to render tissues transparent by removing lipids-e.g., 3DISCO; 3) Aqueous-Based (Ke et al., 2013; Kuwajima et al., 2013; Konno and Okazaki, 2018): these methods use water-based solutions for tissue clearing-e.g., SeeDB; 4) Acrylamide-Based (Yang et al., 2014; Treweek et al., 2015; Hsiao et al., 2023): methods based on acrylamide hydrogel embedding for tissue transparency-e.g., PACT; 5) Miscellaneous (Susaki et al.,

2014; Tang et al., 2017; Bekkouche et al., 2020): methods that do not fit into the above categories-e.g., CUBIC and RapiClear. The advantages and disadvantages of different tissue-clearing methods vary based on their fundamental principles and technologies. For a detailed overview, refer to Table 1.

### Application and observation of tissue-clearing methods in skin

However, how to apply these techniques to skin tissue has yet to be explored. Previous studies employed gene-edited mice along with modified tissue transparency techniques such as CUBIC (Christ and Jakus, 2023) and BABB (Foster et al., 2019) to independently investigate the tissue structure of lymphatic vessels and fibroblasts in murine skin. Moreover, the examination of human skin involved the utilization of the active clarity technique-pressure related efficient and stable transfer of macromolecules into organs (ACT-PRESTO), enabling the visualization and quantitative analysis of epidermal melanocytes and nerve fibers through three-dimensional imaging (Kim et al., 2022a,b). Additionally, the interaction between engineered nanomaterials (ENMs) and the skin barrier was explored by the iDISCO method (Touloumes et al., 2020).

In our study, RapiClear was used on the hairy/hairless skin of rat feet and mouse ears after immunofluorescence staining. In this way, we could

**Table 1.** Lists of common clearing reagents and their usage characteristics.

	Applicable tissues and organs	Technical method	Advantages	Disadvantages
CLARITY	Brain, Spinal Cord, Heart, Kidneys, Liver, Lungs, Pancreas, Intestines, Skin, Whole bodies of small animals	Hydrophilic Tissue-Clearing Methods	1, Preservation of molecular and structural integrity; 2, Compatibility with multiple labeling techniques; 3, Three-dimensional imaging capabilities.	1, Complex, time-consuming process; 2, Potential for tissue damage and protein loss; 3, Limited penetration of antibodies and stains.
3DISCO	Brain, Spinal Cord, Mammary Glands, Kidneys, Lungs, Pancreas, Immune Organs, Tumors, Whole bodies of small animals	Hydrophobic Tissue-Clearing Methods	1, Rapid and efficient clearing; 2, High-resolution and deep tissue imaging; 3, Versatility across different tissue types and species.	1, Tissue shrinkage and deformation; 2, Use of toxic and flammable solvents; 3, Incompatibility with fluorescent proteins.
SeeDB	Brain, Eye, Mammary Glands, Tumors	Aqueous-Based Tissue-Clearing Methods	1, High optical transparency and minimal tissue shrinkage; 2, Compatibility with fluorescent proteins and immunostaining; 3, Simple and non-toxic procedure.	1, Limited clearing depth for larger samples; 2, Prolonged clearing time; 3, Potential for incomplete lipid removal.
PACT	Brain, Spinal Cord, Kidneys, Lungs, Whole bodies of small animals	Acrylamide-Based Tissue-Clearing Methods	1, Enhanced tissue clearing speed; 2, Preservation of structural integrity; 3, Compatibility with whole-organ and whole-body imaging.	1, Long clearing times; 2, Incomplete penetration of clearing agents; 3, Potential for tissue swelling and distortion.
CUBIC	Brain (Human and Marmoset), Kidneys, Whole bodies of small animals	Miscellaneous Tissue-Clearing Methods	1, Deep tissue penetration and high transparency; 2, Versatility across various tissue types; 3, Compatibility with multiple staining and imaging techniques.	1, Long processing times; 2, Potential tissue swelling; 3, Chemical handling and safety concerns.
RapiClear	Brain, Heart, Kidneys, Liver, Lungs, Pancreas, Spleen, Intestines, Lymph Nodes, Bones, Whole embryos, and small animals	Miscellaneous Tissue-Clearing Methods	1, Rapid and efficient clearing; 2, High optical clarity and compatibility with fluorescent imaging; 3, Versatility across various tissue types and organisms.	1, Limited clearing depth for larger samples; 2, Potential for fluorescence quenching; 3, Constraints on long-term storage.

observe the distribution of nerve fibers, blood vessels, and lymphatic vessels in these skin tissues in morphological detail. Notably, it is the correct choice to obtain high-resolution images from thick skin sections and whole-mount skin tissues (Figs. 1, 2). Although several kinds of tissue-clearing methods were available (Table 1), the clearing process with RapiClear is simple and can be accomplished rapidly within a matter of hours (Rulands et al., 2018; Cai et al., 2023). Given the effect of rapid clearing and the compatibility with immunofluorescence staining, the RapiClear strategy has been widely applied across various types of tissues (Table 1).

After conducting triple-fluorescence staining, nerve fibers, blood vessels, and lymphatic vessels were distinctly marked with calcitonin gene-related peptide (CGRP), phalloidin, and lymphatic vessel endothelial hyaluronan receptor 1 (LYVE1), respectively, in both hairy and hairless skin areas (Fig. 1). The application of the clearing process allowed for deeper imaging of CGRP-positive nerve fibers, phalloidin-positive blood vessels, and LYVE1-positive lymphatic vessels, enabling the capture of comprehensive structural details of the skin. The subsequent 3D reconstruction of these tissues made it easier to map their distribution. It was observed that CGRP-positive nerve fibers extended from the subcutaneous layer through the dermis and reached the epidermis. In the subcutaneous layer, these fibers grouped into bundles, branched within the dermis, and eventually spread into the epidermis. In contrast, the phalloidin-positive blood vessels and LYVE1-positive lymphatic vessels were primarily located in the subcutaneous tissue and dermis. Typically, the CGRP-positive nerve fibers either ran parallel to or encircled the blood vessels, collectively forming a three-dimensional network in both hairy and hairless skin regions.

In addition, we also employed the RapiClear method to achieve transparency in the auricular skin of the mouse. Through the utilization of multiple immunofluorescent staining techniques, we provided a morphological distribution of nerve fibers, blood vessels, and lymphatic vessels marked with protein gene product 9.5 (PGP 9.5), cluster of differentiation 31 (CD31), and LYVE1 (Fig. 2). From the whole-mount auricular skin, we observed that they were widely distributed from the basal to the peripheral region of the auricle. The nerve bundles primarily displayed straight-type branches aligned with large blood vessels, while their branches formed complex vascular networks. In contrast, the lymphatic networks originated from lymphatic capillaries characterized by "blind-ended" tubes. From a three-dimensional perspective, the proximity and interconnectedness of neural, vascular, and lymphatic tissue elements within the auricular skin become more apparent. It is reasonable to propose that these elements work together in response to auricular stimulation. This speculation has the potential to provide fresh insights into the anatomical basis of ear acupuncture or

auriculotherapy.

### **Challenges and limitations of tissue-clearing methods in skin tissue**

In the realm of tissue-clearing methods, its predominant usage resides within neuroscience research (Lai et al., 2018; Ueda et al., 2020). The synergistic utilization of transgenic mice has empowered researchers to directly visualize intricate neural circuits and connections within the central nervous system (Winnubst et al., 2019; McCreedy et al., 2021). However, beyond its conventional application, our practical endeavors have unveiled its promising potential in investigating the structure and morphology of the skin (Wang et al., 2022, 2024; Zhang et al., 2023). This technology emerges as a fitting choice for the meticulous examination of cutaneous nerve fibers, blood vessels, and lymphatic vessels in thick skin sections. The conventional challenges associated with tracing cutaneous nerve fibers with extended and intact structures in thin tissue sections are mitigated through the application of tissue-clearing techniques. It is important to underscore that while tissue-clearing technology offers unprecedented insights, it is not without limitations, particularly when it comes to observing cytology in skin tissues (Navarro et al., 1995; Hendrix et al., 2008; Chang et al., 2014; Salz and Driskell, 2017; Yamazaki et al., 2018). Despite these constraints, the expanding horizons of tissue-clearing technology open new avenues for comprehensive investigations into the intricate details of skin structure and its underlying physiology.

In sections of thicker tissues, particularly those densely populated with cells, the close proximity and stacking of cells pose challenges in distinguishing individual cell characteristics. This inherent limitation becomes more pronounced, impeding the effective observation of immune cells. Moreover, the choice of antibodies introduces an additional layer of complexity, as not all antibodies are compatible with thick tissue sections. A further complication arises from the hypothesis that antibodies with smaller molecular weights might offer enhanced effectiveness in immunofluorescence staining within thicker sections. This proposition is grounded in the notion that smaller antibodies may penetrate dense tissues more efficiently, leading to improved staining outcomes (Kim et al., 2022c). Consequently, the intricate process of selecting appropriate antibodies becomes yet another substantial constraint within this method. Balancing the need for effective immunofluorescence staining with the limitations imposed by tissue thickness underscores the complexity inherent in this aspect of the methodology.

For transparent samples, we can take histological images with a confocal microscopy, multiphoton microscopy, and light-sheet fluorescence microscopy. Usually, confocal microscopy, as a cost-effective imaging technique, is used for detailed examination of

## Three-dimensional visualizing skin architecture

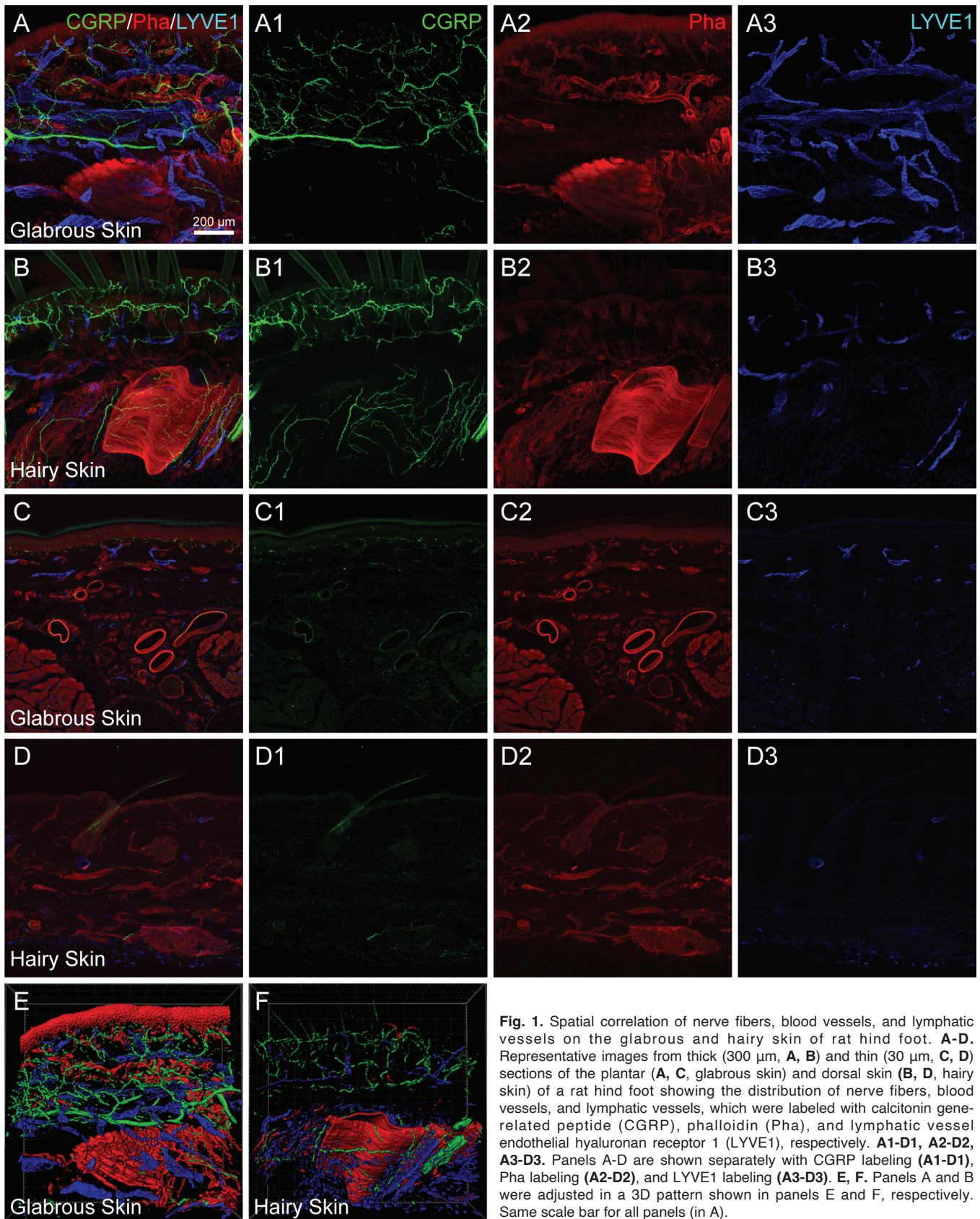


**Fig. 1.** Spatial correlation of nerve fibers, blood vessels, and lymphatic vessels on the glabrous and hairy skin of rat hind foot. **A-D.** Representative images from thick (300 μm, **A, B**) and thin (30 μm, **C, D**) sections of the plantar (**A, C**, glabrous skin) and dorsal skin (**B, D**, hairy skin) of a rat hind foot showing the distribution of nerve fibers, blood vessels, and lymphatic vessels, which were labeled with calcitonin gene-related peptide (CGRP), phalloidin (Pha), and lymphatic vessel endothelial hyaluronan receptor 1 (LYVE1), respectively. **A1-D1**, **A2-D2**, **A3-D3**. Panels **A-D** are shown separately with CGRP labeling (**A1-D1**), Pha labeling (**A2-D2**), and LYVE1 labeling (**A3-D3**). **E, F.** Panels **A** and **B** were adjusted in a 3D pattern shown in panels **E** and **F**, respectively. Same scale bar for all panels (in **A**).

### Three-dimensional visualizing skin architecture

thin sections within a range of 300  $\mu\text{m}$  thickness (Schiffmann et al., 2020; Cui et al., 2021; Sun et al., 2021). In contrast, multiphoton microscopy is more

effective for imaging thicker samples by using near-infrared light to penetrate the tissues deeply (Blanc et al., 2021; Drakhlis et al., 2021). Light-sheet fluorescence

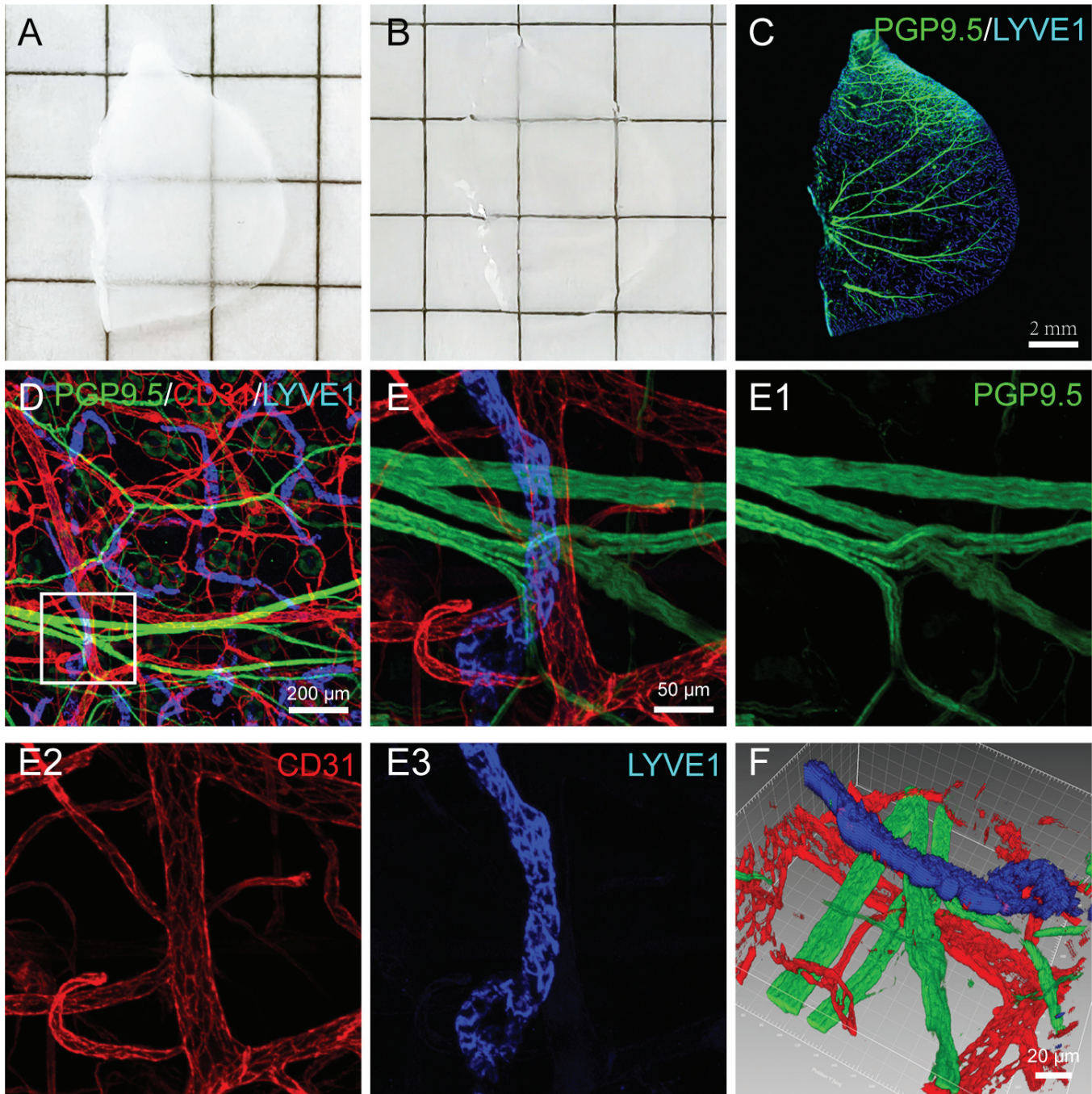


**Fig. 2.** The distribution relationship of nerve fibers, blood vessels, and lymphatic vessels on the auricular skin of mouse. **A, B.** Outside view of the auricular skin before (**A**) and after clearing (**B**). **C.** Montage view of the auricular skin showing the distribution of neural labeling with protein gene product 9.5 (PGP 9.5) and lymphatic labeling with lymphatic vessel endothelial hyaluronan receptor 1 (LYVE1). **D.** Representative image of the auricular skin showing the spatial correlation of neural labeling with PGP 9.5, vascular labeling with cluster of differentiation 31 (CD31), and lymphatic labeling with LYVE1. **E.** Higher magnification photographs from panel D (box-indicated region). **E1-E3.** Panel E was shown separately with PGP 9.5 labeling (**E1**), CD31 labeling (**E2**), and LYVE1 labeling (**E3**). Same scale bar for E-E3 (in E). **F.** Panel E further adjusted in a three-dimensional pattern with oblique directions.

microscopy, as a new-generation imaging technique, has been frequently used to quickly image whole organisms in the fields of developmental biology and neuroscience (Abadie et al., 2018; Wang et al., 2020). To effectively obtain high-quality images from the cleared tissues, organs, or whole organisms, we can select a suitable imaging technique according to their advantages and disadvantages.

Despite the prevalent challenges and limitations, the incorporation of transparency technology for observing skin morphology represents a significant milestone in scientific pursuits. This innovative approach serves as a catalyst for a more exhaustive examination of the circulatory and nervous system distribution within the intricate landscape of the skin. The incorporation of three-dimensional reconstruction techniques further amplifies our capacity to garner nuanced insights into the multifaceted functions of skin tissue. This pioneering application of transparency technology not only transcends conventional barriers but also offers a transformative lens through which we can explore and understand the dynamic interplay of biological structures within the skin. By providing a holistic view of the circulatory and nervous systems in a three-dimensional space, this breakthrough contributes significantly to advancing our comprehension of the complex functions and interactions inherent in skin physiology.

---

*Acknowledgements.* This work was funded by the Innovation Team and Talents Cultivation Program of the National Administration of Traditional Chinese Medicine (No. ZYCYXTD-D-202202) and the Fundamental Research Funds for the Central public welfare research institutes (No. ZZ-YC2023007).

---

## References

- Abadie S., Jaret C., Colombelli J., Chaput B., David A., Grolleau J.L., Bedos P., Lobjois V., Descargues P. and Rouquette J. (2018). 3D imaging of cleared human skin biopsies using light-sheet microscopy: A new way to visualize in-depth skin structure. *Skin Res. Technol.* 24, 294-303.
- Bekkouche B.M.B., Fritz H.K.M., Rigosi E. and O'Carroll D.C. (2020). Comparison of transparency and shrinkage during clearing of insect brains using media with tunable refractive index. *Front. Neuroanat.* 14, 599282.
- Blanc T., Goudin N., Zaidan M., Traore M.G., Bienaime F., Turinsky L., Garbay S., Nguyen C., Burtin M., Friedlander G., Terzi F. and Pontoglio M. (2021). Three-dimensional architecture of nephrons in the normal and cystic kidney. *Kidney. Int.* 99, 632-645.
- Cai X.J., Han M.Y., Lou F.Z., Sun Y., Yin Q.Q., Sun L.B., Wang Z.K., Li X.X., Zhou H., Xu Z.Y., Wang H., Deng S.Y., Zheng X.C., Zhang T.Y., Li Q., Zhou B. and Wang H.L. (2023). Tenascin C+ papillary fibroblasts facilitate neuro-immune interaction in a mouse model of psoriasis. *Nat. Commun.* 14, 2004.
- Chang H., Wang Y.S., Wu H. and Nathans J. (2014). Flat mount imaging of mouse skin and its application to the analysis of hair follicle patterning and sensory axon morphology. *J. Vis. Exp.* 88, e51749.
- Christ C. and Jakus Z. (2023). Visualization of organ-specific lymphatic growth: An efficient approach to labeling molecular markers in cleared tissues. *Int. J. Mol. Sci.* 24, 5075.
- Chung K. and Deisseroth K. (2013). CLARITY for mapping the nervous system. *Nat. Methods* 10, 508-513.
- Chung K., Wallace J., Kim S.Y., Kalyanasundaram S., Andalman A.S., Davidson T.J., Mirzabekov J.J., Zalocusky K.A., Mattis J., Denisin A.K., Pak S., Bernstein H., Ramakrishnan C., Grosenick L., Gradinaru V. and Deisseroth K. (2013). Structural and molecular interrogation of intact biological systems. *Nature* 497, 332-337.
- Cui X., Jing J., Wu R., Cao Q., Li F.F., Li K., Wang S.R., Yu L.Q., Schwartz G., Shi H.D., Xue B.Z. and Shi H. (2021). Adipose tissue-derived neurotrophic factor 3 regulates sympathetic innervation and thermogenesis in adipose tissue. *Nat. Commun.* 12, 5362.
- Drakhlis L., Biswanath S., Farr C.M., Lupanow V., Teske J., Ritzenhoff K., Franke A., Manstein F., Bolesani E., Kempf H., Liebscher S., Schenke-Layland K., Hegermann J., Nolte L., Meyer H., de la Roche J., Thiemann S., Wahl-Schott C., Martin U. and Zweigerdt R. (2021). Human heart-forming organoids recapitulate early heart and foregut development. *Nat. Biotechnol.* 39, 737-746.
- Ertürk A., Becker K., Jähring N., Mauch C.P., Hojer C.D., Egen J.G., Hellal F., Bradke F., Sheng M. and Dodt H.U. (2012). Three-dimensional imaging of solvent-cleared organs using 3DISCO. *Nat. Protoc.* 7, 1983-1995.
- Foster D.S., Nguyen A.T., Chinta M., Salhotra A., Jones R.E., Mascharak S., Titan A.L., Ransom R.C., da Silva O.L., Foley E., Briger E. and Longaker M.T. (2019). A clearing technique to enhance endogenous fluorophores in skin and soft tissue. *Sci. Rep.* 9, 15791.
- Hendrix S., Picker B., Liezmann C. and Peters E.M. (2008). Skin and hair follicle innervation in experimental models: A guide for the exact and reproducible evaluation of neuronal plasticity. *Exp. Dermatol.* 17, 214-227.
- Hsiao F.T., Chien H.J., Chou Y.H., Peng S.J., Chung M.H., Huang T.H., Lo L.W., Shen C.N., Chang H.P., Lee C.Y., Chen C.C., Jeng Y.M., Tien Y.W. and Tang S.C. (2023). Transparent tissue in solid state for solvent-free and antifade 3D imaging. *Nat. Commun.* 14, 3395.
- Ke M.T., Fujimoto S. and Imai T. (2013). SeeDB: A simple and morphology-preserving optical clearing agent for neuronal circuit reconstruction. *Nat. Neurosci.* 16, 1154-1161.
- Kim D.H., Lee S.J., Seo S.H., Ahn H.H., Kim B.J., Sun W. and Rhyu I.J. (2022a). Three-dimensional imaging for the analysis of human epidermal melanocytes. *Pigment. Cell. Melanoma Res.* 35, 534-538.
- Kim D.H., Lee S.J., Kim J.H., Park S.J., Seo S.H., Ahn H.H., Sun W., Kim B.J. and Rhyu I.J. (2022b). Whole structural reconstruction and quantification of epidermal innervation through the suction blister method and skin-clearing technique. *Sci. Rep.* 12, 13596.
- Kim H.J., Kim J., Choi J. and Sun W. (2022c). Chemical fluorescence-based dye staining for 3-dimensional histopathology analysis. *Anim. Cells. Syst.* 26, 45-51.
- Kirchner K.N., Li H.L., Denton A.R., Harrod S.B., Mactutus C.F. and Booze R.M. (2020). A hydrophobic tissue clearing method for rat brain tissue. *J. Vis. Exp.* 166, 10.3791/61821.
- Konno A. and Okazaki S. (2018). Aqueous-based tissue clearing in crustaceans. *Zoological Lett.* 4, 13.
- Kuwajima T., Sitko A.A., Bhansali P., Jurgens C., Guido W. and Mason C. (2013). ClearT: A detergent- and solvent-free clearing method for neuronal and non-neuronal tissue. *Development* 140, 1364-1368.

### Three-dimensional visualizing skin architecture

- Lai H.M., Liu A.K.L., Ng H.H.M., Goldfinger M.H., Chau T.W., DeFelice J., Tilley B.S., Wong W.M., Wu W. and Gentleman S.M. (2018). Next generation histology methods for three-dimensional imaging of fresh and archival human brain tissues. *Nat. Commun.* 9, 1066.
- McCreeedy D.A., Jalufka F.L., Platt M.E. and Min S.W. (2021). Passive clearing and 3D lightsheet imaging of the intact and injured spinal cord in mice. *Front. Cell. Neurosci.* 15, 684792.
- Navarro X., Verdú E., Wendelschafer-Crabb G. and Kennedy W.R. (1995). Innervation of cutaneous structures in the mouse hind paw: A confocal microscopy immunohistochemical study. *J. Neurosci. Res.* 41, 111-120.
- Pan C.C., Cai R.Y., Quacquarelli F.P., Ghasemigharagoz A., Loubopoulos A., Matryba P., Plesnila N., Dichgans M., Hellal F. and Ertürk A. (2016). Shrinkage-mediated imaging of entire organs and organisms using uDISCO. *Nat. Methods* 13, 859-867.
- Peng Y.C., Lin Y.C., Hung Y.L., Fu C.C., Chang M.D., Lin Y.Y. and Chou T.Y. (2022). Rapid histological assessment of prostate specimens in the three-dimensional space by hydrophilic tissue clearing and confocal microscopy. *J. Histochem. Cytochem.* 70, 597-608.
- Pomaville M.B. and Wright K.M. (2021). Immunohistochemical and genetic labeling of hairy and glabrous skin innervation. *Curr. Protoc.* 1, e121.
- Renier N., Wu Z.H., Simon D.J., Yang J., Ariel P. and Tessier-Lavigne M. (2014). iDISCO: A simple, rapid method to immunolabel large tissue samples for volume imaging. *Cell* 159, 896-910.
- Richardson D.S. and Lichtman J.W. (2015). Clarifying tissue clearing. *Cell* 162, 246-257.
- Rulands S., Lescroart F., Chabab S., Hindley C.J., Prior N., Sznurkowska, M.K., Huch M., Philpott A., Blanpain C. and Simons B.D. (2018). Universality of clone dynamics during tissue development. *Nat. Phys.* 14, 469-474.
- Salz L. and Driskell R.R. (2017). Horizontal whole mount: A novel processing and imaging protocol for thick, three-dimensional tissue cross-sections of skin. *J. Vis. Exp.* 126, 56106.
- Schiffmann L.M., Werthenbach J.P., Heintges-Kleinhofer F., Seeger J.M., Fritsch M., Günther S.D., Willenborg S., Brodesser S., Lucas C., Jüngst C., Albert M.C., Schorn F., Witt A., Moraes C.T., Bruns C.J., Pasparakis M., Krönke M., Eming S.A., Coutelle O. and Kashkar H. (2020). Mitochondrial respiration controls neoangiogenesis during wound healing and tumour growth. *Nat. Commun.* 11, 3653.
- Sun Q.C., Tiziana P., Khan A.U.M., Heuveline V. and Gretz N. (2021). A simple optical tissue clearing pipeline for 3D vasculature imaging of the mediastinal organs in mice. *Int. J. Exp. Pathol.* 102, 218-227.
- Susaki E.A. and Ueda H.R. (2016). Whole-body and whole-organ clearing and imaging techniques with single-cell resolution: Toward organism-level systems biology in mammals. *Cell. Chem. Biol.* 23, 137-157.
- Susaki E.A., Tainaka K., Perrin D., Kishino F., Tawara T., Watanabe T.M., Yokoyama C., Onoe H., Eguchi M., Yamaguchi S., Abe T., Kiyonari H., Shimizu Y., Miyawaki A., Yokota H. and Ueda H.R. (2014). Whole-brain imaging with single-cell resolution using chemical cocktails and computational analysis. *Cell* 157, 726-739.
- Tang S.C., Shen C.N., Lin P.Y., Peng S.J., Chien H.J., Chou Y.H., Chamberlain C.E. and Pasricha P.J. (2017). Pancreatic neuro-insular network in young mice revealed by 3D panoramic histology. *Diabetologia* 61, 158-167.
- Tian T. and Li X.G. (2020). Applications of tissue clearing in the spinal cord. *Eur. J. Neurosci.* 52, 4019-4036.
- Tian T., Yang Z.Y. and Li X.G. (2021). Tissue clearing technique: Recent progress and biomedical applications. *J. Anat.* 238, 489-507.
- Touloumes G.J., Ardoña H.A.M., Casalino E.K., Zimmerman J.F., Chantre C.O., Bitounis D., Demokritou P. and Parker K.K. (2020). Mapping 2D- and 3D-distributions of metal/metal oxide nanoparticles within cleared human ex vivo skin tissues. *NanoImpact* 17, 100208.
- Treweek J.B., Chan K.Y., Flytzanis N.C., Yang B., Deverman B.E., Greenbaum A., Lignell A., Xiao C., Cai L., Ladinsky M.S., Bjorkman P.J., Fowlkes C.C. and Gradinaru V. (2015). Whole-body tissue stabilization and selective extractions via tissue-hydrogel hybrids for high-resolution intact circuit mapping and phenotyping. *Nat. Protoc.* 10, 1860-1896.
- Ueda H.R., Ertürk A., Chung K., Gradinaru V., Chédotal A., Tomancak P. and Keller P.J. (2020). Tissue clearing and its applications in neuroscience. *Nat. Rev. Neurosci.* 21, 61-79.
- Wang Y.T., Dai G.Y., Gu Z.L., Liu G.P., Tang K., Pan Y.H., Chen Y.J., Lin X., Wu N., Chen H.S., Feng S., Qiu S., Sun H.D., Li Q., Xu C., Mao Y.N., Zhang Y.E., Khaitovich P., Wang Y.L., Liu Q.X., Han J.D.J., Shao Z., Wei G., Xu C., Jing N. and Li H.P. (2020). Accelerated evolution of an Lhx2 enhancer shapes mammalian social hierarchies. *Cell Res.* 30, 408-420.
- Wang X.Y., Cao W.Y., Shi J.T., Zhang X.N., Qu Z.Y., Xu D.S., Wan H.Y., Su Y.S., He W., Jing X.H. and Bai W.Z. (2022). Demonstrating hairy and glabrous skin innervation in a 3D pattern using multiple fluorescent staining and tissue clearing approaches. *J. Vis. Exp.* 183, doi 10.3791/63807.
- Wang Y.Q., Su Y.X., Wang J., Zhang K.W., Zhang W.J., Cui J.J., Liu Y.H., Wang X.Y. and Bai W.Z. (2024). Networks of nerve fibers, and blood and lymphatic vessels in the mouse auricle: The structural basis of ear acupuncture. *Med. Acupunct.* 36, 79-86.
- Winnubst J., Bas E., Ferreira T.A., Wu Z. and Economu M.N. (2019). Reconstruction of 1,000 projection neurons reveals new cell types and organization of long-range connectivity in the mouse brain. *Cell* 179, 268-281.
- Yamazaki T., Li W.L. and Mukoyama Y.S. (2018). Whole-mount confocal microscopy for adult ear skin: A model system to study neuro-vascular branching morphogenesis and immune cell distribution. *J. Vis. Exp.* 133, 57406.
- Yang B., Treweek J.B., Kulkarni R.P., Deverman B.E., Chen C.K., Lubeck E., Shah S., Cai L. and Gradinaru V. (2014). Single-cell phenotyping within transparent intact tissue through whole-body clearing. *Cell* 158, 945-958.
- Zhang K.W., Guo Y.T., Su Y.X., Wang Y.Q., Cui J.J., Zhang J.L., Wang J. and Bai W.Z. (2023). Tissue clearing for three-dimensional visualization of the auricular neurovascular network. *Prog. Biochem. Biophys.* 50, 1473-1479.
- Zhu X.P., Huang L.M., Zheng Y., Song Y., Xu Q., Wang J., Si K., Duan S. and Gong W. (2019). Ultrafast optical clearing method for three-dimensional imaging with cellular resolution. *Proc. Natl. Acad. Sci. USA* 116, 11480-11489.